



**Michigan
Technological
University**

Michigan Technological University
Digital Commons @ Michigan Tech

Dissertations, Master's Theses and Master's Reports

2019

Comparative Study and Design of Economical Sound Intensity Probe

Karan Gundre

Michigan Technological University, gundre@mtu.edu

Copyright 2019 Karan Gundre

Recommended Citation

Gundre, Karan, "Comparative Study and Design of Economical Sound Intensity Probe", Open Access Master's Report, Michigan Technological University, 2019.
<https://doi.org/10.37099/mtu.dc.etdr/798>

Follow this and additional works at: <https://digitalcommons.mtu.edu/etdr>



Part of the [Acoustics, Dynamics, and Controls Commons](#)

COMPARATIVE STUDY AND DESIGN OF ECONOMICAL SOUND INTENSITY
PROBE

By

Karan Gundre

A REPORT

Submitted in partial fulfillment of the requirements for the degree of

MASTER OF SCIENCE

In Mechanical Engineering

MICHIGAN TECHNOLOGICAL UNIVERSITY

2019

© 2019 Karan Gundre

This report has been approved in partial fulfillment of the requirements for the Degree of
MASTER OF SCIENCE in Mechanical Engineering.

Department of Mechanical Engineering – Engineering Mechanics

Report Advisor: *Dr. Andrew Barnard*

Committee Member: *Dr. Jason Blough*

Committee Member: *Dr. James DeClerck*

Department Chair: *Dr. William W. Predebon*

Table of Contents

List of figures	v
List of tables.....	vii
Acknowledgements	viii
Abstract	ix
1 Introduction.....	1
2 Background	3
2.1 Intensity Probe Transducer Configurations.....	3
2.2 Cross-Spectral Method of Measuring Intensity.....	4
2.3 Measurement Apparatus.....	5
2.4 Errors in Measurement	8
2.4.1 Finite Difference Approximation Errors.....	9
2.4.2 Phase Mismatch Errors	10
2.4.3 Microphone Errors	11
3 Methodology	13
3.1 Phase Calibration.....	13
3.2 Intensity Calculation.....	14

3.3	Data Acquisition.....	15
3.4	Probe Unit.....	16
3.5	Spacers.....	18
3.6	LabVIEW Code.....	19
3.7	Cost.....	25
4	Testing and Results	26
5	Conclusion	36
6	Reference List	37

List of figures

Figure 2-1. Face-to-face mic configuration with 1/2" mic and 50-mm spacer mounted on probe, and 12-mm, 25-mm and 100-mm spacers shown to the side.....	6
Figure 2-2. Effective frequency ranges for various mic and spacer configurations (image reproduced [8]).....	8
Figure 2-3. Pressure gradient estimation for low and high frequency waves	9
Figure 2-4. Condenser microphone showing diaphragm and pressure equalization vent (image reproduced from Jacobsen et al [9])	12
Figure 3-1. Side-view of 3D-Printed Phase Calibrator with a US quarter for scale (top); and front-view cross-section of the phase calibrator (bottom)	13
Figure 3-2. PCB 2-channel signal conditioner and A-to-D converter (Model 458B39) ...	16
Figure 3-3. Custom probe design with 3-D printed mic holders and aluminum base with a 50-mm spacer	17
Figure 3-4. Custom probe design that is entirely 3-D printed	17
Figure 3-5. CAD model of vented spacer designed for use with array microphones on custom probe	19
Figure 3-6. Data Flow in Phase Calibration VI	20

Figure 3-7. Data Flow in Intensity Measurement VI.....	20
Figure 3-8. Startup VI of LabVIEW program for intensity measurement.....	22
Figure 3-9. Amplitude calibration VI of LabVIEW program for measuring intensity.....	23
Figure 3-10. Phase calibration VI of LabVIEW program for measuring intensity	24
Figure 3-11. Intensity Measurement VI of LabVIEW program for measuring intensity ..	24
Figure 4-1. B&K calibrated sound source	26
Figure 4-2. GRAS probe with 50-mm spacer	27
Figure 4-3. Custom probe with 50-mm spacer	27
Figure 4-4. Phase mismatch recorded between the two microphones on custom probe ...	28
Figure 4-5. GRAS vs Custom probe for 12-mm spacer configuration	29
Figure 4-6. GRAS vs Custom Probe (zoomed in) for 12-mm configuration.....	30
Figure 4-7. Difference in intensities between two probes after octave-band filtering.....	30
Figure 4-8. GRAS vs Custom probes for 50-mm spacers	31
Figure 4-9. GRAS vs Custom probes (zoomed in) for 50-mm configuration	32
Figure 4-10. Difference in intensities between probes after octave-band filtering.....	32

List of tables

Table 1. Cost breakdown of custom intensity probe.....	25
--	----

Acknowledgements

I would like to thank everyone who has helped me throughout my research. First, I would like to thank Dr. Andrew Barnard for giving me the opportunity to work on this project and his unlimited support and guidance. I would also like to thank Dr. Jason Blough and Dr. James DeClerck for their support and agreeing to be on my defense committee. Additionally, I would like to thank Dr. Barnard, Dr. Blough and Dr. DeClerck again, along with Chuck Van Karsen, for all the unparalleled knowledge and wisdom they have imparted to me in and out of class during my time here.

I would like to thank Sunit Girdhar for his help in setting up experiments and brainstorming. I would also like to acknowledge Adit Manurkar who designed the prototype of the original 3D-printed phase calibrator. Additionally, I would also like to acknowledge Alexander Lurie, Matthew Anderson, Nathaniel Evenhouse and Swapnil Pandey in their contribution in designing one of the 3D-printed intensity probes. Finally, I would like to thank my fellow research group members for their frequent words of wisdom.

Abstract

The theory of sound intensity measurement using the two-microphone method was first developed in the late 1970s. Even though the measurements were limited by the technology of the time, the theory was straight-forward and considerable attention was given to improving precision during testing or post-processing. With the development of modern equipment, however, the focus shifted to the apparatus. The commercial intensity probes available today have microphones that are already phase-matched. This eliminates the need for correction during or post-testing as a majority of the errors are minimized before any data is even collected. Although such intensity probes facilitate taking precise measurements, they have a major drawback – cost. Additionally, not only are phase-matched microphones expensive to manufacture but they are also hard to replace.

This report explores an intensity measurement technique that enables the use of current, inexpensive equipment along with a custom LabVIEW code. Phase and amplitudes are corrected using dedicated, handheld calibrators. The phase calibrator and the intensity probe are manufactured using in-house rapid prototyping to bring down the cost. Custom LabVIEW code is developed that calculates sound intensity while dealing with phase mismatch between the two relatively inexpensive microphones. Furthermore, the custom intensity probe is compared with a commercially available probe and the measurement readings are discussed.

1 Introduction

Sound intensity is defined as the acoustic power passing through a given area on a measurement surface near or around the sound source. It is given in Watts per meters squared (W/m^2). In its most basic form, sound intensity is the product of sound pressure and particle velocity. The principles for measurement of sound intensity were first developed in the late 1970s and rudimentary techniques followed soon after. Measuring sound pressure has been always been relatively easy. Transducers that measure sound pressure – microphones – are readily available at a reasonable cost. However, measuring particle velocity is complicated. Unlike microphones that have been available for more than a century, transducers that measure particle velocity have only been developed in the early 2000s. Although these transducers have been significantly developed since they were first introduced, they are relatively hard to come by and costly.

These techniques of measuring sound intensity were actively developed in the '80s and '90s, when the equipment available was not as sophisticated as it is now. However, with the advent of newer equipment that acquired and processed data quickly and with fewer inherent errors, the focus shifted to improving test apparatus, which gave virtually error-free results, although at a much higher monetary cost.

This project explores a technique which was popular before sophisticated equipment was available. The technique enables use of inexpensive apparatus to bring down the cost of

measurement. Modern software is used to compensate for the inherent errors brought in by the equipment.

2 Background

2.1 Intensity Probe Transducer Configurations

Intensity is calculated from the product of sound pressure and particle velocity. These two factors – sound pressure and particle velocity – dictate the type of measurements required in the two techniques as the transducers required to directly measure each quantity are different. Intensity is a vector quantity, meaning it has magnitude and direction. The magnitude is measured using two microphones positioned next to each other in a face-to-face or side-to-side arrangement [1, 2]. There are also techniques involving a greater number of microphones that can sense direction as well, but these are not discussed here.

Within the two-microphone technique domain, there are two types – pressure-pressure transducer pair (P-P) and pressure-velocity transducer pair (P-U). P-P technique uses a pressure microphone pair while P-U technique uses one pressure microphone and one particle velocity microphone.

The main concern in intensity measurement is estimating the particle velocity. Measuring sound pressure but measuring particle velocity is not. Jacobsen et al. compare the two techniques of measuring sound intensity using standard ½” pressure microphones and Microflown particle velocity transducer [3]. The Microflown particle velocity transducer has two heated, thin, closely-spaced wires of silicon nitride coated with platinum. The air passing over these wires cools each wire separately causing a temperature gradient, which is then used to calculate the acoustic particle velocity. These transducers are not affected

by the sources that cause errors in pressure transducers and are thus more accurate in estimating particle velocity in a laboratory environment [3].

2.2 Cross-Spectral Method of Measuring Intensity

Intensity is simply the product of sound pressure and particle velocity. This is given by:

$$I = \frac{1}{2} \text{Re}[pu^*] \quad (1)$$

Where I is the intensity, p is the sound pressure and u is the particle velocity and $*$ denotes the conjugate term. Also, p and u are complex quantities. The presence of the particle velocity term makes this frequency-domain expression unfeasible for measurement purposes as particle velocity cannot be measured directly without a particle velocity transducer. It is thus estimated using finite difference approximation of the pressures from the two microphones in a P-P probe. This finite difference approximation is evaluated further to derive an expression where the intensity is estimated from the cross-spectral density of the two pressure. Waser et al, Chung and Fahy independently derived an expression for sound intensity in terms of cross-spectrum of the two microphone channels [4-6]. This expression is valid for all sound fields – near/far and free/reverb. By performing finite difference approximation and fast Fourier transform on equation 1, the expression for sound intensity is given in the frequency domain as [4-7]:

$$I(\omega) = \frac{\text{Im}[G_{12}]}{\omega \rho \Delta r} \quad (2)$$

Where, ω is the frequency in rad/sec, $I(\omega)$ is the intensity as a function of frequency, ω , $\text{Im}[G_{12}]$ is the imaginary part of the cross-spectrum of channels 1 & 2, ρ is the density of air, and, Δr is the microphone separation distance.

Equation 2 simplifies the process of measuring sound intensity by a great deal as the only quantity that needs to be measured in the process is the cross-spectrum of the two channels. Cross-spectrum measurements are straightforward as all modern data acquisition systems have frequency domain measurement capabilities.

For the cross-spectrum in equation 2, the order of the channels matter. In $[G_{12}]$, the linear spectrum of channel 1 is multiplied with conjugate of linear spectrum of channel 2. However, if the conjugate of linear spectrum of channel 1 is used instead of 2, a minus sign has to be put in front of the equation. Since,

$$\text{Im} \{S_1 S_2^*\} = - \text{Im} \{S_1^* S_2\}. \quad (3)$$

2.3 Measurement Apparatus

The basic components of a P-P sound intensity probe are two pressure microphones, a solid spacer, a probe to hold the microphones and spacer, an amplifier and a data acquisition system. Figure 2-1 shows the face-to-face probe arrangement, where the solid black cylinder mounted on the probe is a 25-mm spacer and it is being held between two 1/2" microphones that are in a face-to-face arrangement.



Figure 2-1. Face-to-face mic configuration with 1/2" mic and 50-mm spacer mounted on probe, and 12-mm, 25-mm and 100-mm spacers shown to the side

The microphones can be in one of three configurations – face-to-face, side-to-side or end-to-end. Of these, the face-to-face configuration with a solid spacer is preferred, as the spacer protects the measurements from scattering errors that may decrease accuracy of the measurement [1, 3]. Using spacers with other arrangements is not recommended. Additionally, the microphone size used along with a length of spacer also influences the measured data. Microphone sizes in themselves do not necessarily have any significant effect on the measurement but the microphone spacer has a great effect. This is because the length of spacer is directly proportional to the upper frequency limit of the measurement and inversely proportional to the phase mismatch between the two microphones. So, an optimum length of spacer needs to be selected. Equation 4 gives the generally accepted condition for selecting a spacer.

$$k \cdot \Delta r \ll 1 \quad (4)$$

Where, k is the wavenumber (ratio of frequency and speed of sound in air), and, Δr is the microphone separation distance.

Jacobsen et al. [1] observed that for a ½” microphone with a 12-mm spacer, the upper limit of frequency is 5 kHz and the error is less than 1 dB while for a ¼” microphone with a 6-mm spacer, the upper limit is 10 kHz. Although the latter configuration has a relatively higher frequency range, the noise from ¼” increases the error in measurement and the short spacer raises the lower limit of the frequency range. Jacobsen et al. assert that an optimum spacer length is equal to one microphone diameter.

For most applications, a configuration of ½” microphones with 12-mm spacer is optimum because the configuration has good low frequency accuracy and a realistic upper frequency limit [1, 3, 8, 9]. In practice, the equipment for which intensity measurements are carried out do not have significant high frequency content [10]. Figure 2-2 shows effective frequency ranges for different configurations of microphone and spacers.

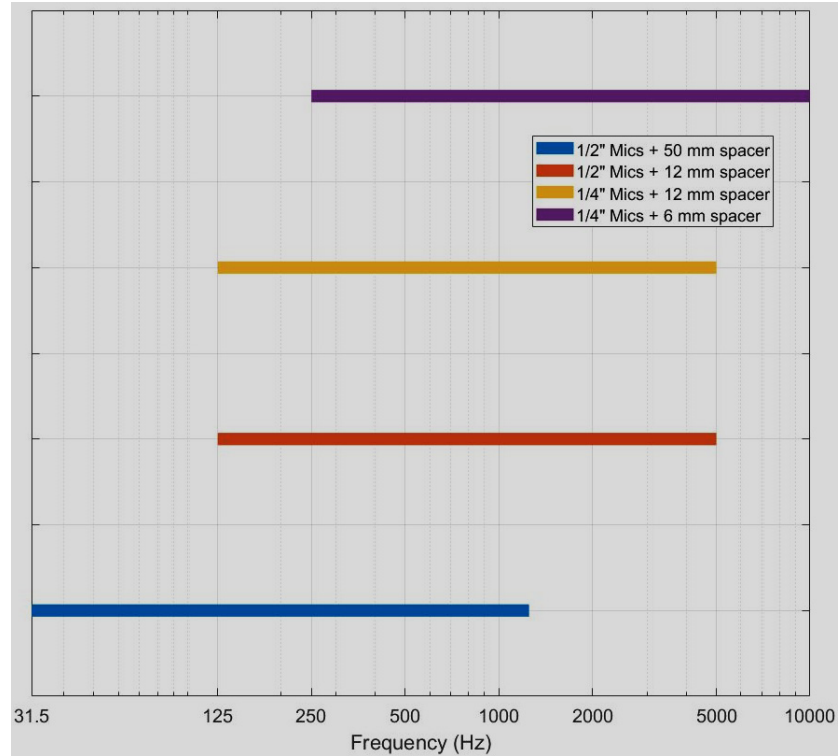


Figure 2-2. Effective frequency ranges for various mic and spacer configurations (image reproduced [8])

2.4 Errors in Measurement

The three main sources of errors are finite difference approximation, phase mismatch between channels or microphones and microphone errors. The finite difference approximation errors set the upper limit of the frequency range and the phase mismatch errors set the lower limit [8].

2.4.1 Finite Difference Approximation Errors

These are errors in estimating particle velocity using finite difference approximation. A pressure gradient between pressure signals of the two microphones is estimated and using a version of the Euler's equation, the particle velocity is obtained. The accuracy of this approximation, however, is dependent on the frequency of the input wave. Figure 2-3 show the approximation in a high and low frequency waves. At low frequency, the estimated and actual gradients have a decent agreement but with increasing frequency, the accuracy decreases considerably.

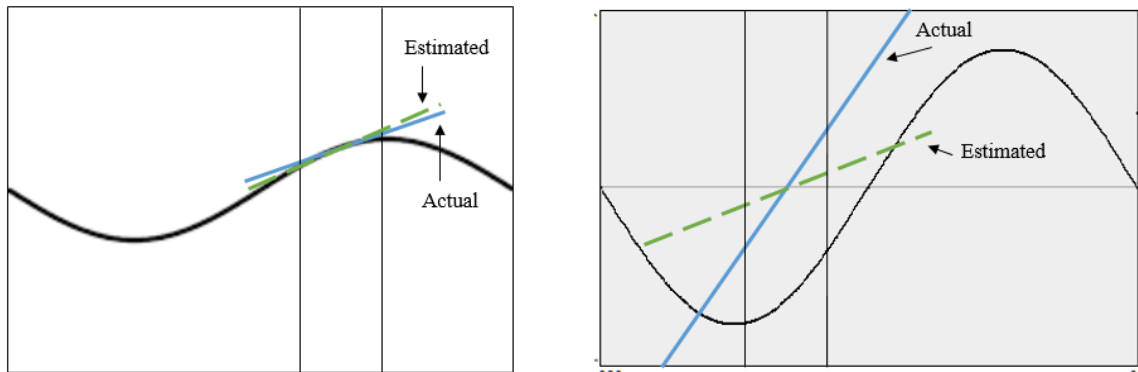


Figure 2-3. Pressure gradient estimation for low and high frequency waves

Error due to finite difference approximation increases with frequency but can be avoided by satisfying the condition given in equation 4 [11]. In other words, choosing an appropriate separation distance can help avoid the error. It should be noted that the separation distance is the distance between the diaphragms of the two microphones and not the length of spacer separating the two microphones externally.

2.4.2 Phase Mismatch Errors

Phase mismatch is the foremost contributor to errors in measuring sound intensity. As phase mismatch directly affects the cross-spectral density being measured, the entire data set obtained is very sensitive to errors due to phase mismatch. Jacobsen [12] emphasizes that, contrary to popular belief, the errors due to phase mismatch are not exclusive to low frequencies and that they affect the entire frequency range. Additionally, errors due to phase mismatch are inversely proportional to the separation distance between microphones.

There are two primary techniques of minimizing errors due to phase mismatch – circuit-switching and offsetting phase of one channel from the other with phase calibration. Since most of the research done in the sound intensity measurement field has been in the late 20th century, when equipment sophisticated enough to perform the latter technique were unavailable, researchers focused on the circuit-switching technique [4, 5, 8, 9, 11].

Circuit-switching technique requires the measurements to be taken twice; taking the second set of measurements with the circuits ‘switched’ or interchanged. There is some misconception about whether the term ‘circuits’ refers to only the microphones or entire channels. Most researchers only switch the microphones after the first measurement. This is advantageous since this way the phase mismatch between the amplifier and data acquisition device channels are averaged out and they do not affect the measured data. Precise results are obtained from using the circuit-switching technique [5]. However, this

technique requires twice the time for measurement which might not always be desirable [11].

Phase calibration of the microphones before making measurements allows the tests to be done only once without compromising on precision. In this technique, the microphones are snugly fit in a phase calibrator that has a speaker inside it. The speaker plays random noise (or pseudo random noise) in the enclosed cavity. Because of the way the microphones are positioned in the cavity, the phase difference between them, as a function of frequency, is obtained. This phase function is then offset from one of the microphones thereby getting rid of the phase mismatch. The gain is also calibrated in the same way [11].

2.4.3 Microphone Errors

Condenser or pressure microphones use a diaphragm that moves when sound pressure waves hit it. This movement of the diaphragm is converted to voltage and represented in appropriate units to give the sound pressure level. On the inside of the diaphragm, there is a pressure equalization vent that maintains ambient pressure behind the diaphragm. A pressure gradient across the two sides of the diaphragm would give rise to bias errors. Figure 2-4 shows the diaphragm and pressure equalization vent in a condenser microphone. These small air cavities on the front and rear sides of the diaphragm act as if filled with fluid. These have a resistance and an impedance, and can cause appreciable bias errors at low frequencies in strongly reactive fields [9]. However, these bias errors can be predicted and corrected. Additionally, avoiding near-field effects further help in reducing the bias errors.

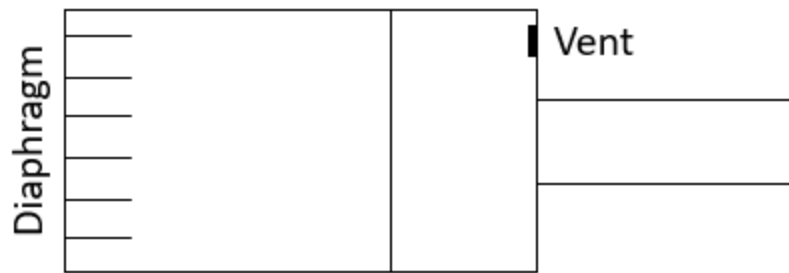


Figure 2-4. Condenser microphone showing diaphragm and pressure equalization vent

(image reproduced from Jacobsen et al [9])

Also inducing errors in measurement is the inconsistent spread of sensitivity across the diaphragm and non-symmetrical cavity pressure. These affect the directional response of the microphones which consequently induces errors in measurement. These errors increase with frequency.

The only way to avoid these errors during testing is to use an appropriate solid spacer with a symmetric probe configuration. Face-to-face arrangement with a solid spacer has significantly fewer errors than the side-to-side arrangement [2]. Additionally, the damping of the diaphragm also affects the measurement accuracy [13]. Since these are errors at the manufacturing level, these cannot be eliminated by physically modifying the setup. But these can be minimized to an insignificant level with averaging techniques.

3 Methodology

3.1 Phase Calibration

The most important aspect of the intensity probe is phase match between the two microphones. Which is why manufacturers spend thousands of dollars in the production of each phase-matched microphone. The precision lost in not using sophisticated equipment is compensated for by using a custom LabVIEW code and a phase calibrator to phase-calibrate the microphones. Figure 3-1 shows the phase calibrator housing and its cross-section.

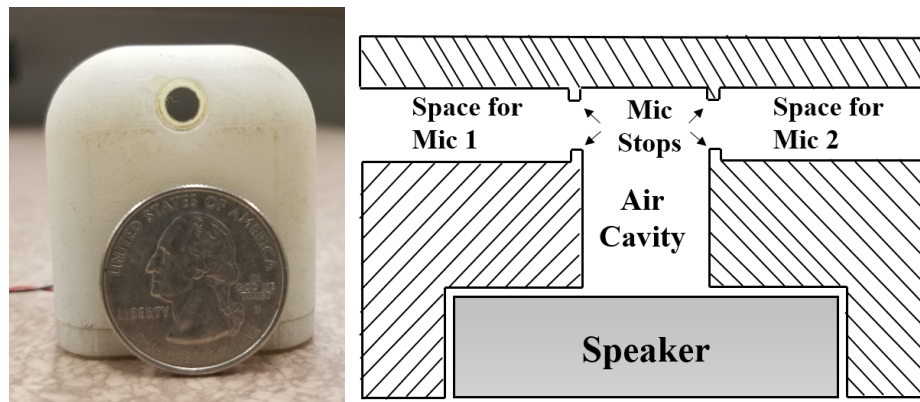


Figure 3-1. Side-view of 3D-Printed Phase Calibrator with a US quarter for scale (top);
and front-view cross-section of the phase calibrator (bottom)

The phase calibrator has a 3-D printed housing with an inexpensive 1" moving coil speaker inside that outputs random white noise. The phase calibrator is designed in such a way that the sound pressure at the two ends where mics are inserted into the calibrator is the same. This ensures that at any given point in time during calibration, both the microphones are

receiving the same input. Using this, the relative phase mismatch only between the two channels is recorded and stored. This relative mismatch is later offset from the crosspower before calculating intensity using the cross-spectrum calculation.

All this is achieved from the LabVIEW code which performs these computations in real-time. Along with the phase calibration, the LabVIEW program also has provisions for amplitude calibration, which is just as important.

3.2 Intensity Calculation

Once the phase mismatch is recorded, the array containing phase information siphons off that information to intensity measurement section of the code. There are two main aspects to measuring intensity – measuring cross-spectrum and offsetting phase. The expression for cross-power of two input channels, 1 & 2, is given by:

$$S_{12} = A_{12}(\omega) \cdot e^{j[\varphi_{12}(\omega)]} \quad (5)$$

Where, S_{12} is the cross-power between channels 1 & 2, $A_{12}(\omega)$ is the frequency dependent amplitude, and $\varphi_{12}(\omega)$ is the frequency dependent phase.

In equation 5, the power of exponent, $\varphi_{12}(\omega)$, contains the phase information. For measurements done using regular phase unmatched microphones, the term also contains the phase error that needs to be removed. This is done by offsetting the relative phase mismatched obtained during the phase calibration. Equation 5 is modified to accommodate the phase correction factor and it is given in equation 6.

The expression for the cross-spectrum between microphones 1 & 2 with the correction for phase mismatch applied is:

$$S_{12} = A_{12}(\omega) \cdot e^{j[\varphi_{12}(\omega) - \varphi_c(\omega)]} \quad (6)$$

Where, $\varphi_c(\omega)$ is the frequency dependent relative phase mismatch between the two channels measured in the phase calibrator. This phase correction procedure is also implemented in real time using LabVIEW code, thereby eliminating the need of using expensive, phase-matched microphones. With the corrected cross-power available, intensity is calculated using equation 2.

3.3 Data Acquisition

The custom design uses a 2-channel USB digital signal conditioner and analog-to-digital converter (PCB Model 458B39) to acquire data. The PCB signal conditioner (shown in figure 3-2) is a compact unit that replaces the need for large data acquisition modules. It connects to the computer via USB and is also relatively inexpensive. The signal conditioner aids in bringing down the cost of the setup while providing decent dual-channel data acquisition capabilities.



Figure 3-2. PCB 2-channel signal conditioner and A-to-D converter (Model 458B39)

3.4 Probe Unit

Rapid prototyping offers the freedom to test out a number of designs without investing significantly. The probe body, phase calibrator housing and spacers are all manufactured using rapid prototyping to further alleviate costs. During the development of the custom probe, two main probe designs were focused on. These are shown in figure 3-3 and figure 3-4.

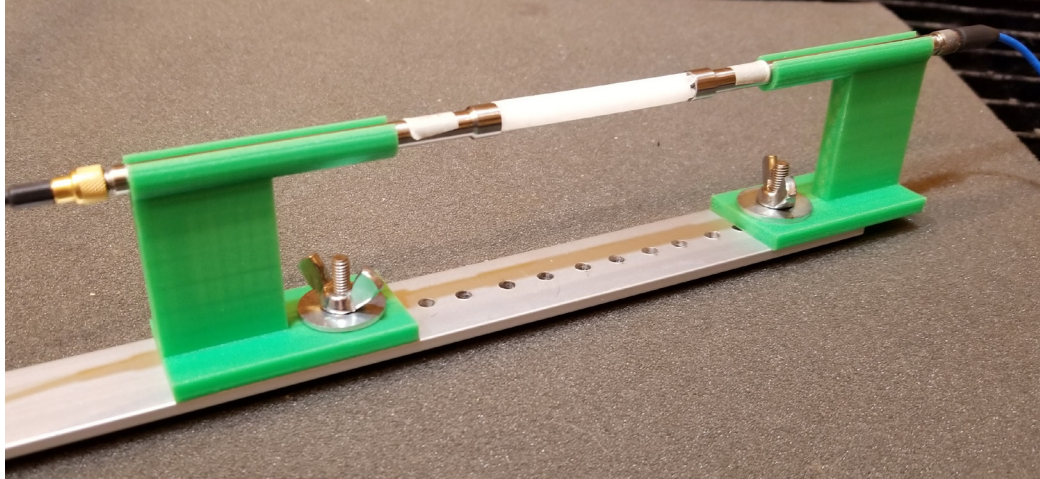


Figure 3-3. Custom probe design with 3-D printed mic holders and aluminum base with a 50-mm spacer

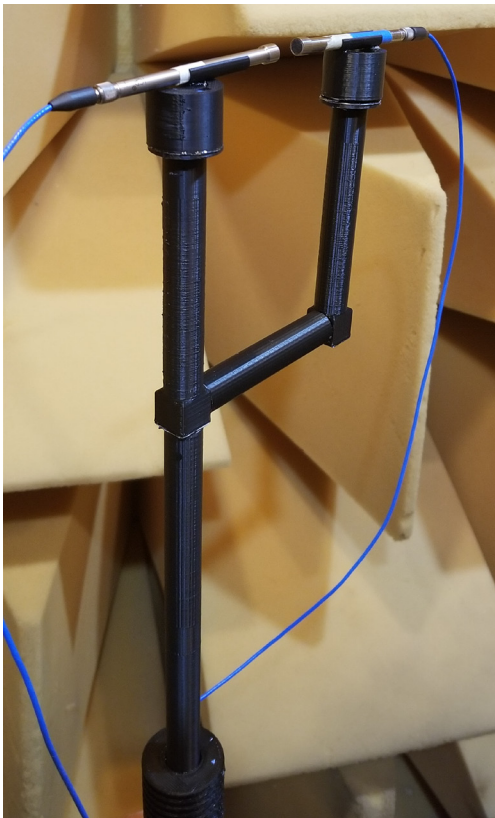


Figure 3-4. Custom probe design that is entirely 3-D printed

Although rapid prototyping, or 3-D printing, offers versatility in terms of designing abstract shapes, the final print is only as good as the printer. So, care needs to be taken where tight tolerances or strength is needed in the design. The probe in figure 3-3 has a metal base with holes to facilitate changing the microphone separation distance while the probe in figure 3-4 has removable adapters (top cylindrical component where mics are mounted) that can be switched out and reprinted according to the separation distance required. Majority of the testing during this project has been done using the former probe.

3.5 Spacers

In the face-to-face P-P technique, the two microphones are quite close together. This closeness results in scattering effects, which are avoided using. The length of the spacer decides the range in which the setup will be free of scattering effects and consequently, the measurements would be good. The commercial probe used – GRAS 50AI – uses microphones that have venting on the sides which enables the use of solid spacers. The microphones being used for the custom probe, however, are array microphones and do not have venting on the sides. Thus, special vented spacers were designed, and 3-D printed for the probe. The CAD model for such a spacer is shown in figure 3-5. These facilitate the entrance of pressure waves into the microphone.

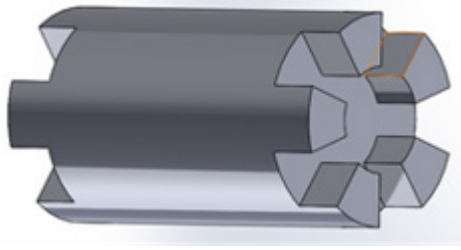


Figure 3-5. CAD model of vented spacer designed for use with array microphones on custom probe

3.6 LabVIEW Code

LabVIEW offers tools to make measurements and calculations simultaneously and in real-time. Using the PCB DAQ with LabVIEW helps uncomplicate the setup as it does not require specialized hardware drivers, like DAQmx or similar, to interface with the USB-enabled DAQ. Figure 3-6 shows a brief overview of the data flow in phase calibration section of the code. After the mics are plugged into the phase calibrator and a random noise input is given, the time signals acquired from each mic are recorded by the LabVIEW code and the crosspower spectrum is calculated for the two channels. From this, the phase information, which is the relative phase mismatch, is extracted. This phase information is saved to an Excel file, for future reference, and is also stored in a Functional Global Variable (FGV).

FGVs are VIs that use loops with uninitialized shift registers to store global data. These help transfer data from one section, or VI, of the LabVIEW code to other while the code is

running. The phase information stored is stored in the FGV temporarily so it can be retrieved and used during the intensity measurement part.

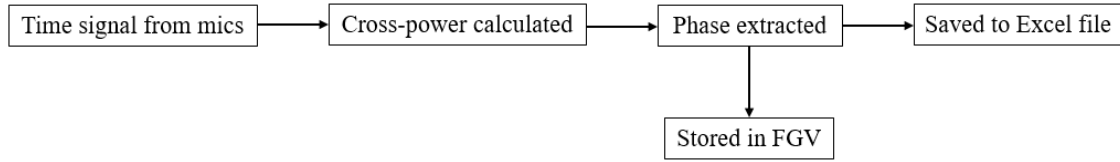


Figure 3-6. Data Flow in Phase Calibration VI

Figure 3-7 shows a brief flow of data in the intensity measurement VI. The time signals from mics are read and crosspower is calculated for the two channels. Considering that the application of this code is for inexpensive, phase-mismatched microphones, the crosspower calculated will include the instrumentation phase mismatch which needs to be offset. Thus, the crosspower is split into amplitude and phase, and the phase information from the phase calibration step is called from the FGV. This is then offset from the phase in the intensity measurement step and then combined with the amplitude to obtain crosspower between the two channels with phase mismatch corrected. Intensity is then calculated from this using the cross-spectral formulation, given in equation 2.

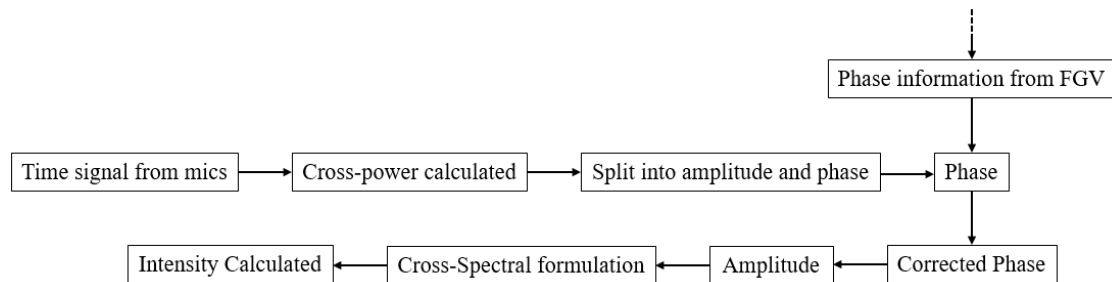


Figure 3-7. Data Flow in Intensity Measurement VI

The LabVIEW code developed is built into an executable and packaged with a LabVIEW Run-Time Engine installer. This package enables the program to be run on any reasonably equipped computer. Figure 3-8 shows the startup VI where the user can choose to phase calibrate, amplitude calibrate or make intensity measurements. The startup VI also allows the user to set few of the acquisition parameters at the beginning and they will remain the same for all processes unless the user wishes to change the parameters.

Figure 3-9 & figure 3-10 show the amplitude and phase calibration VIs, respectively. The 1” speaker in the phase calibrator has a small dynamic range and poor low frequency performance. Thus, the measurements are made for frequency range of 25 Hz – 6 kHz. This range is also in agreement with the spacer limitations. The phase information obtained here is written to an Excel file for future reference and the array is sent to the intensity measurement VI.

Figure 3-11 shows the intensity measurement VI. The VI also has its own settings for sampling parameters that can be tweaked but it should be noted that the phase mismatch will have been recorded for a set of sampling parameters.

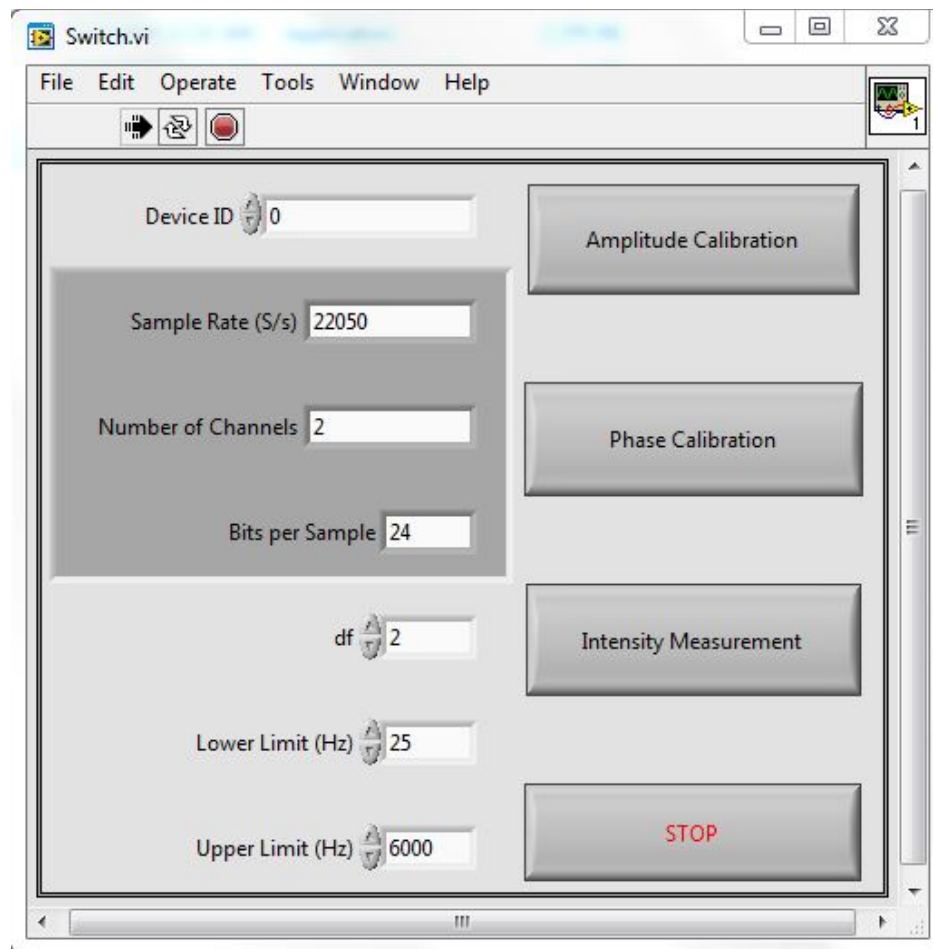


Figure 3-8. Startup VI of LabVIEW program for intensity measurement

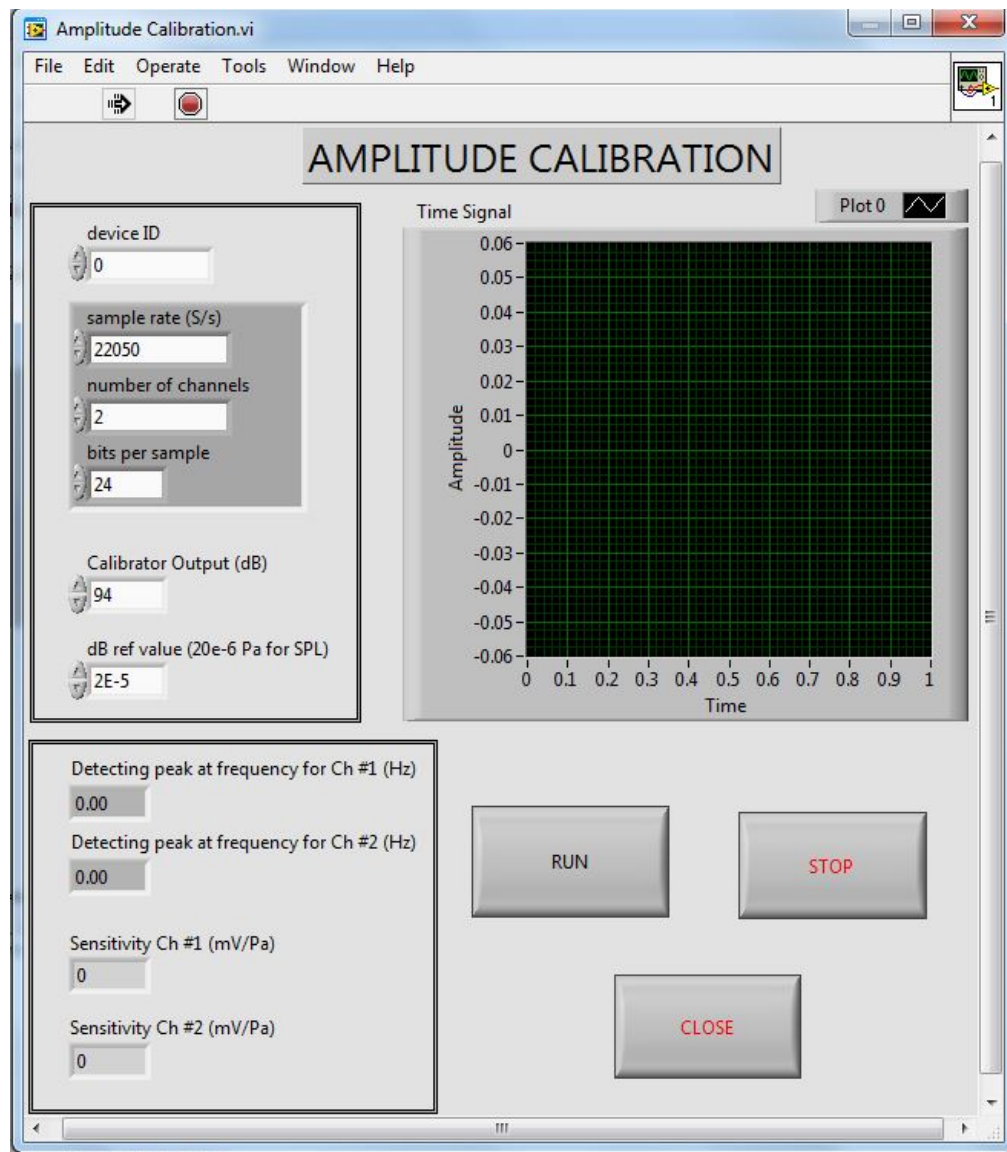


Figure 3-9. Amplitude calibration VI of LabVIEW program for measuring intensity

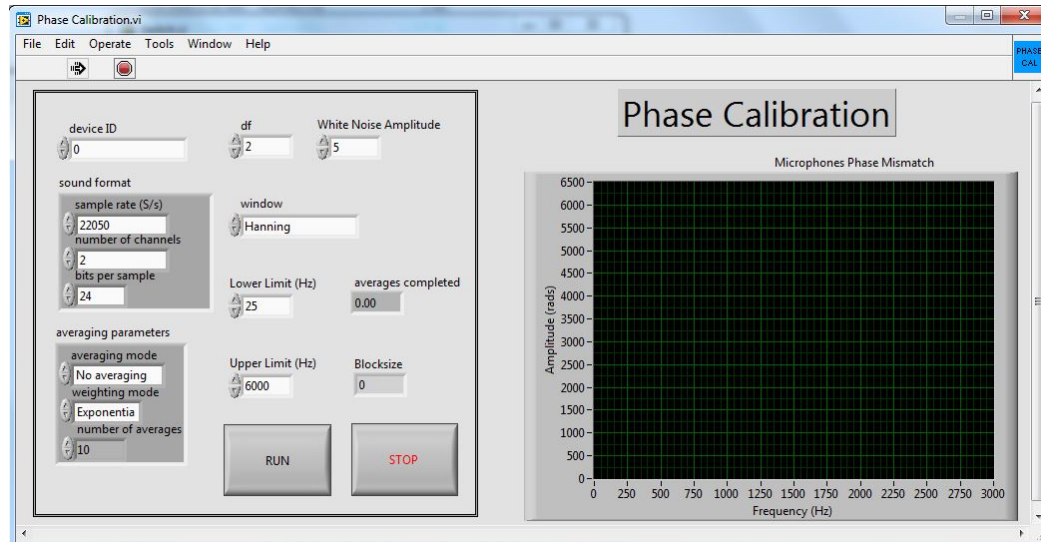


Figure 3-10. Phase calibration VI of LabVIEW program for measuring intensity

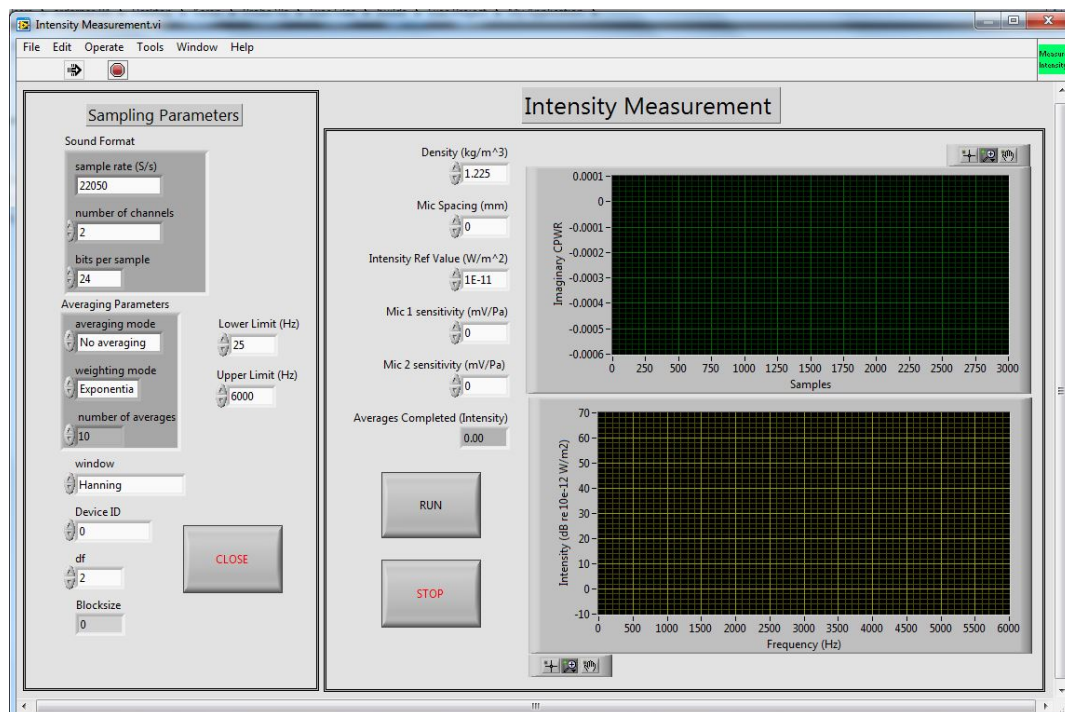


Figure 3-11. Intensity Measurement VI of LabVIEW program for measuring intensity

3.7 Cost

The commercial intensity probe setup uses sophisticated hardware that drives up the cost. This cost may not be inclusive of the data acquisition system that will be required to make measurements. The data acquisition systems can themselves run into tens of thousands of dollars. Additionally, since the hardware is so expensive, it is quite difficult to replace.

In the case of the custom probe, since the accuracy of the measurements of the probe depend mainly on the LabVIEW program, it can use low-cost hardware. Table 1 gives the detailed cost breakdown of the custom intensity probe.

Table 1. Cost breakdown of custom intensity probe

Component		Quantity	Cost per unit	Cost
Phase Calibrator	Amplifier	1	\$22	\$22
	Speaker	1	\$5	\$5
	3D Printed Housing	1	\$25	\$25
Intensity Probe	USB DAQ	1	\$1000	\$1000
	¼" ICP Microphones	2	\$250	\$500
	3D Printed Handle	1	\$15	\$15
Other	Cables	2	\$100	\$100
Total Cost				\$1667

4 Testing and Results

To validate the custom probe, a commercially available probe – GRAS 50AI – is chosen and both the probes are compared directly. The probes measure 3 different outputs from a B&K calibrated power source under the same measurement conditions. This B&K speaker outputs a known amount of energy in a preset octave band. Figure 4-1 shows the source.



Figure 4-1. B&K calibrated sound source

The GRAS probe is paired with an LMS SCADAS XS data acquisition system and the measurements are taken via LMS Test.Lab Spectral Testing module. It is also equipped with $\frac{1}{2}$ " microphones while the custom probe has $\frac{1}{4}$ " microphones. Measurements for 12-mm and 50-mm spacers for both probes are taken. Figure 4-2 shows the GRAS probe with 50-mm spacer and figure 4-3 shows the custom probe with 50-mm spacer.



Figure 4-2. GRAS probe with 50-mm spacer



Figure 4-3. Custom probe with 50-mm spacer

For the custom probe, the first important step is to phase calibrate the microphones. Figure 4-4 shows the phase mismatch recorded.

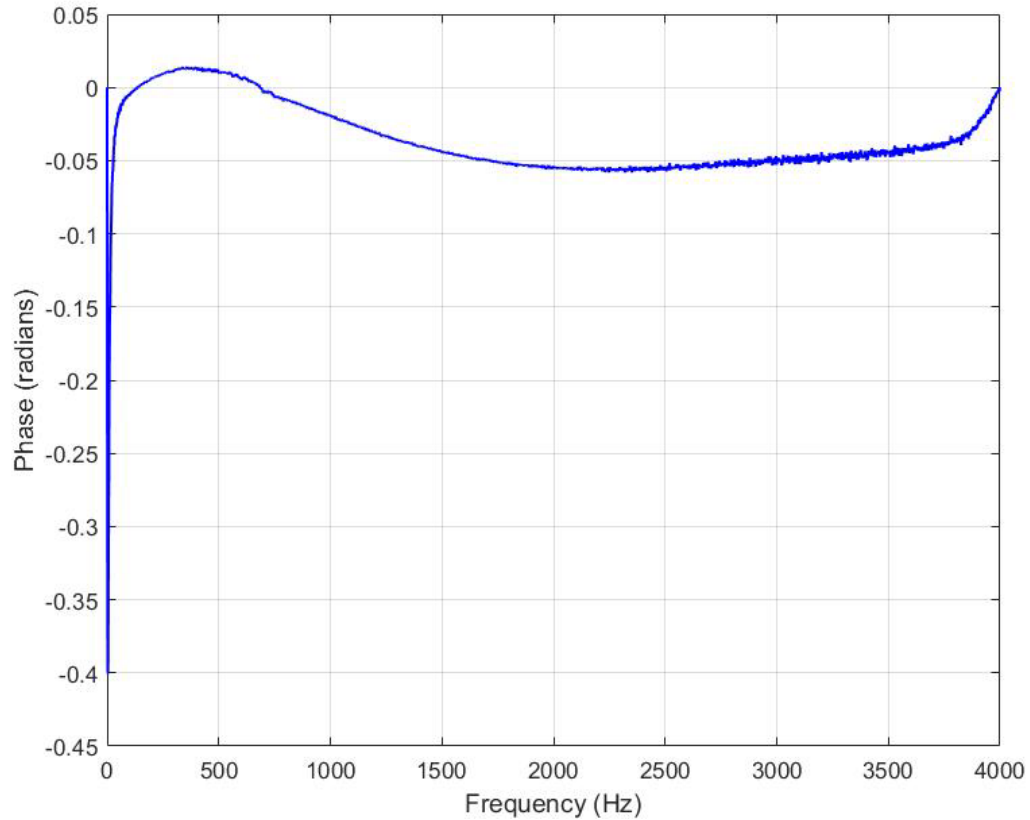


Figure 4-4. Phase mismatch recorded between the two microphones on custom probe

The B&K sound source is set at three different settings and tested for each. The source is focusing its energy in the 500 Hz octave band in one setting, 1 kHz band in other and 2 kHz in the third. Since the spacer-microphone configuration and dynamic range of phase calibrator speaker limited the high frequency content that can be measured to below 6 kHz, the upper limit for measurements is set at 4 kHz. This is done to achieve legal bandwidths on both the data acquisition devices.

Figure 4-5 shows the measurements for 12-mm spacer configuration. Figure 4-6 shows the same plot zoomed in and figure 4-7 shows the difference in intensities between the two probes after octave band filtering. The figures show good agreement between the measurements from two probes in the expected range. The data obtained for frequencies lower than 500 Hz is not good and that also agrees with the limits that using a solid spacer poses.

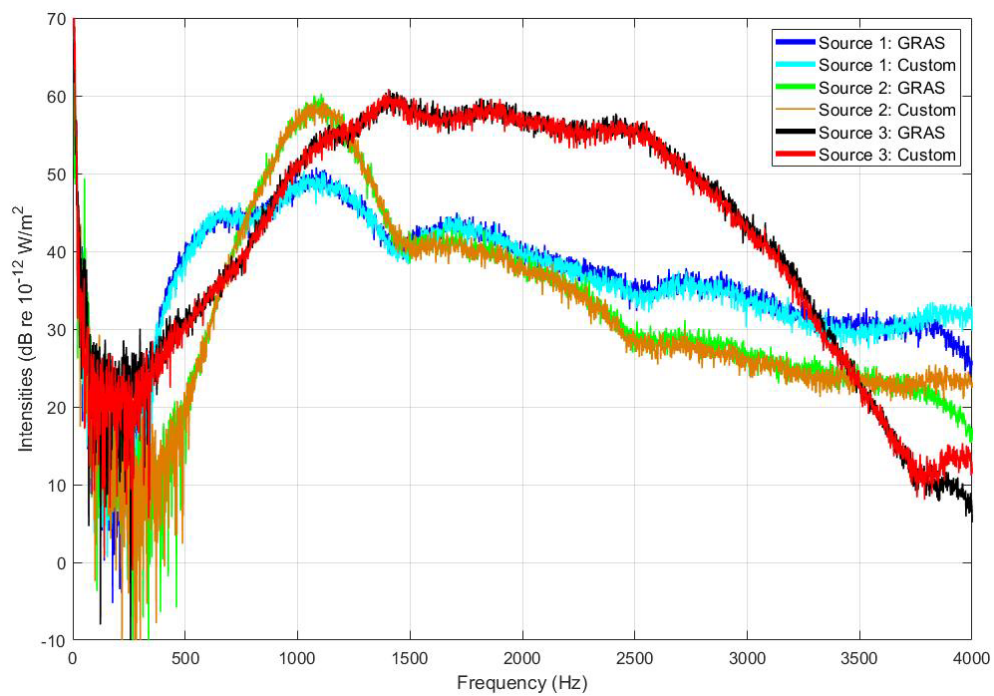


Figure 4-5. GRAS vs Custom probe for 12-mm spacer configuration

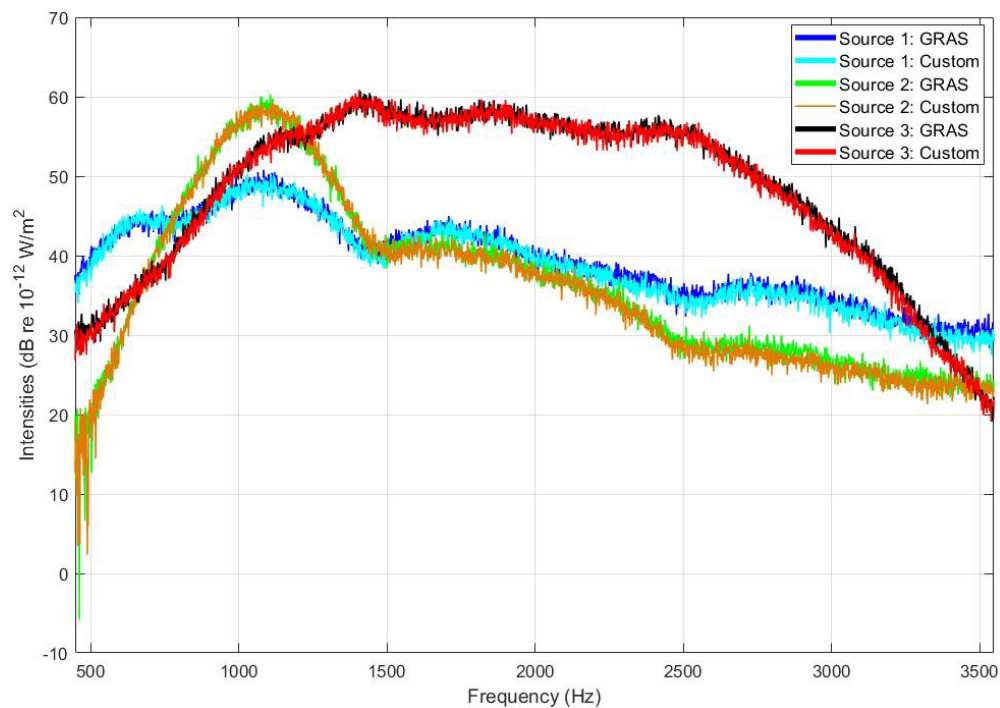


Figure 4-6. GRAS vs Custom Probe (zoomed in) for 12-mm configuration

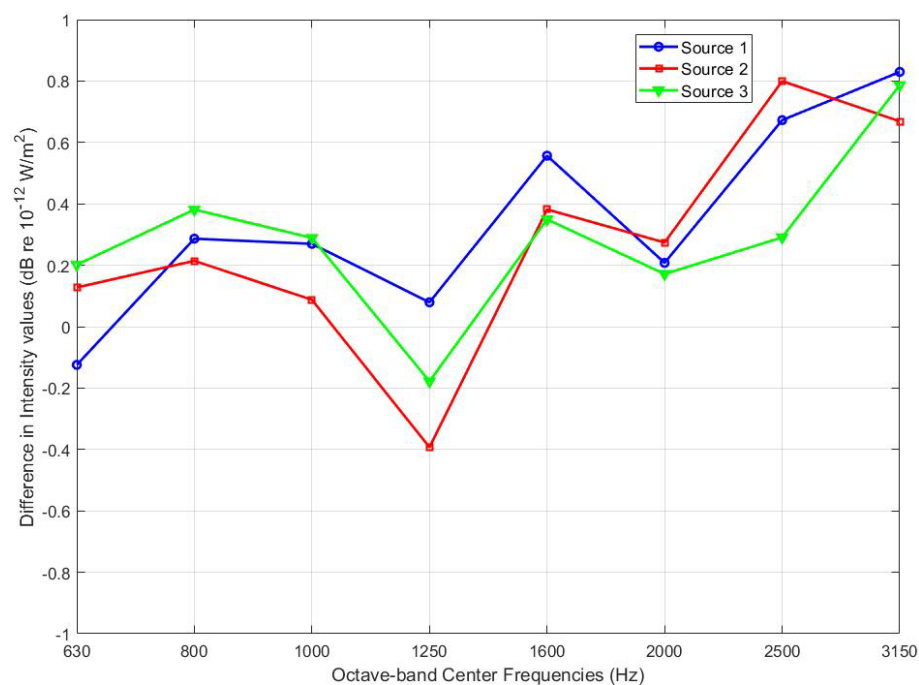


Figure 4-7. Difference in intensities between two probes after octave-band filtering

Figure 4-8 shows the measurements for 50-mm spacer configuration. Figure 4-9 shows the same plot zoomed in and figure 4-10 shows the difference in intensities between the two probes after octave band filtering.

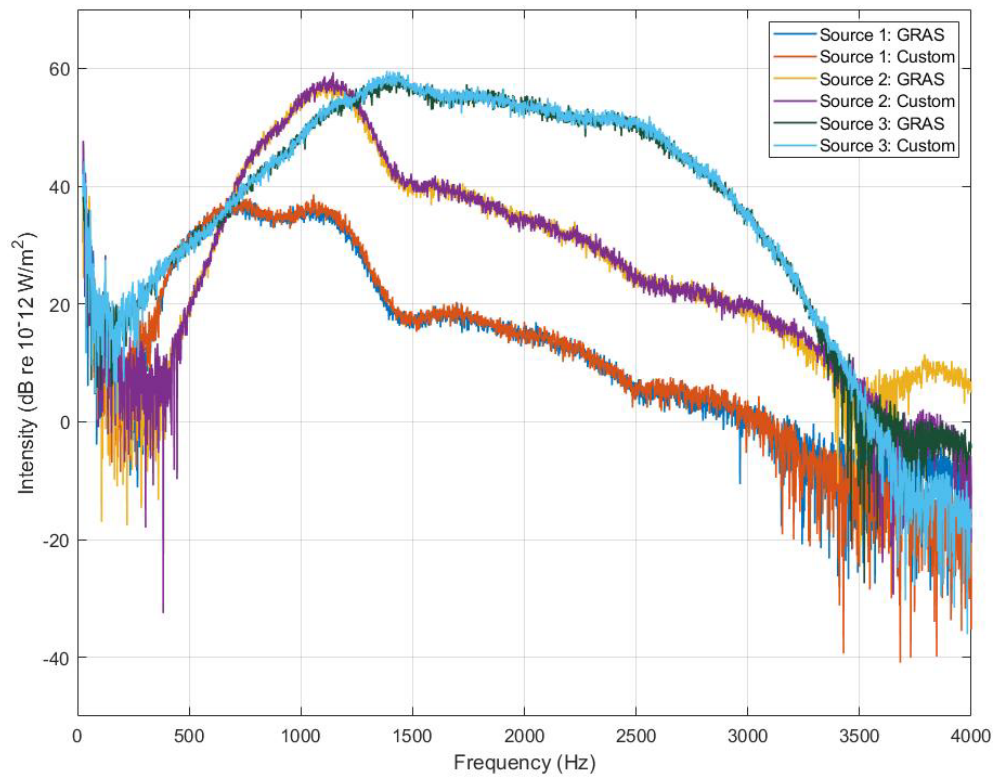


Figure 4-8. GRAS vs Custom probes for 50-mm spacers

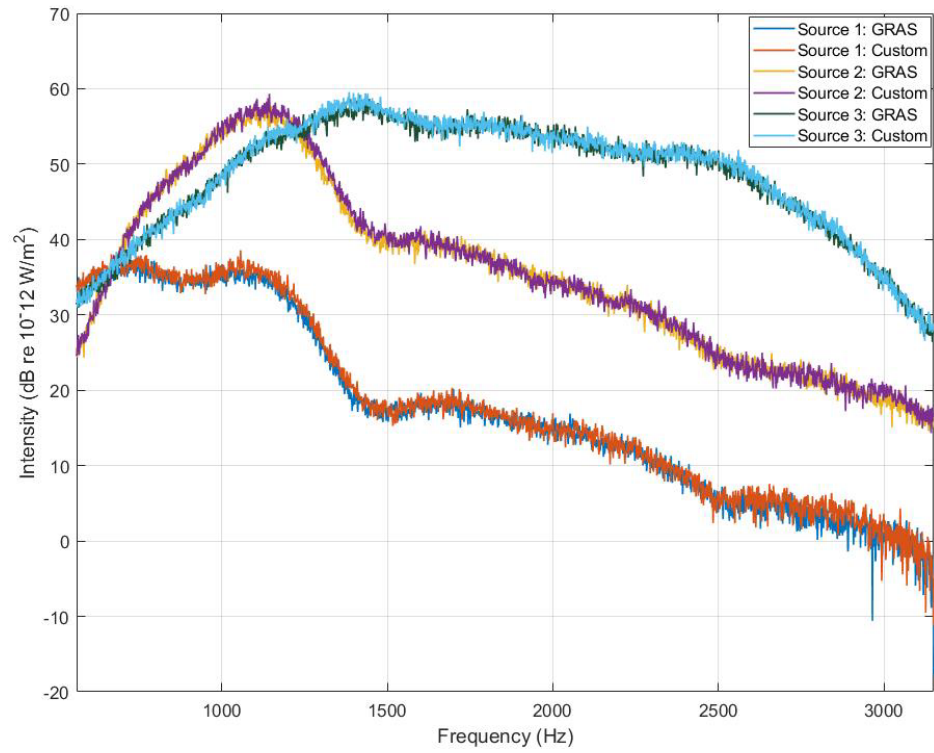


Figure 4-9. GRAS vs Custom probes (zoomed in) for 50-mm configuration

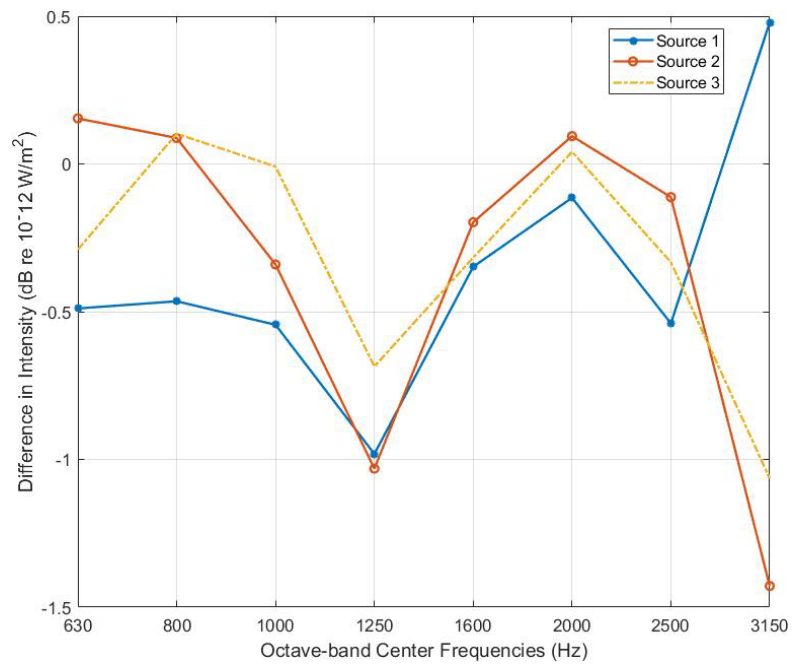


Figure 4-10. Difference in intensities between probes after octave-band filtering

Additionally, to determine the importance of phase matching in intensity measurement, a flat phase mismatch is added to the cross-spectrum data of the GRAS probe measurement for one of the sources. Figure 4-4 shows that phase mismatch in the two channels of the custom probe was around -0.05 radians (2.86°) in the 562-3548 Hz range. As GRAS probe uses phase matched microphones that have negligible phase mismatch, a flat instrumentation phase error of 1° , 3° and 5° was added. The intensity was then calculated in MATLAB using the cross-spectral formulation. Figure 4-11 shows the absolute error in intensity values in the erroneous data with respect to the original GRAS probe data. Figure 4-12 shows the absolute error after one-third octave filtering.

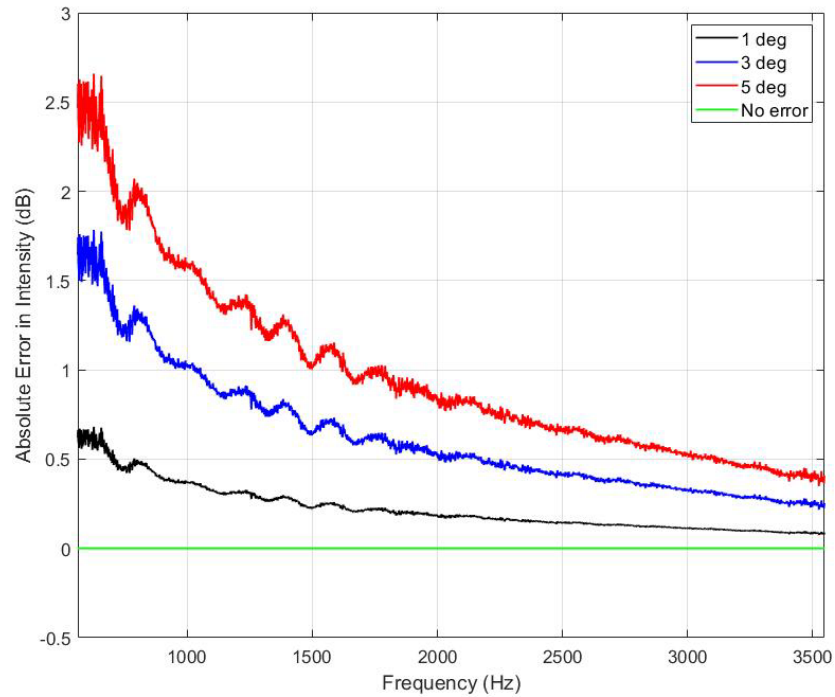


Figure 4-11. Absolute Error in Intensity for 562-3548 Hz range (narrowband)

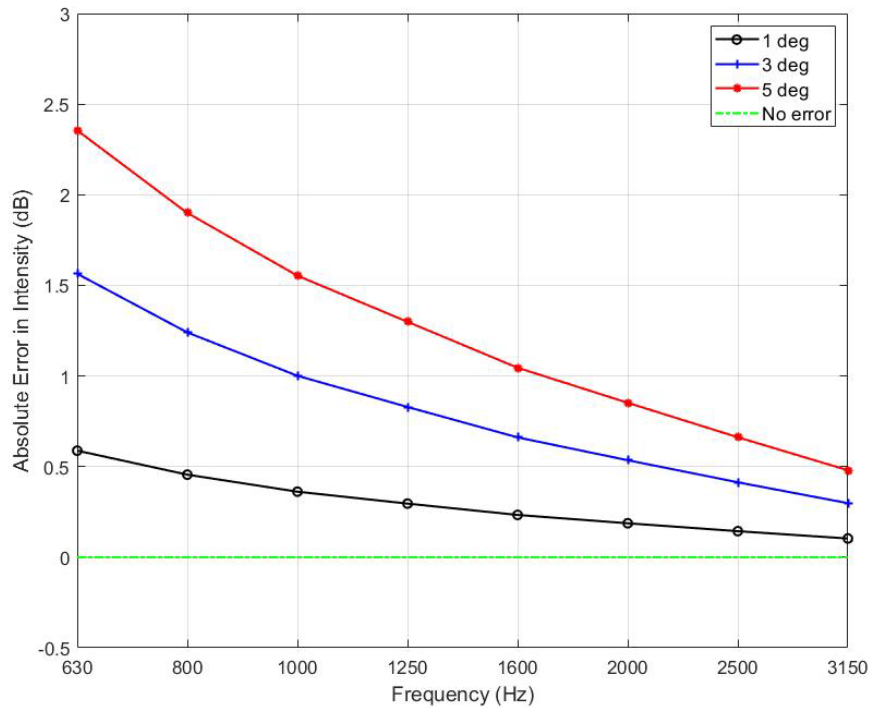


Figure 4-12. Absolute Error in Intensity for One-Third Octave bands

Error due to phase mismatch is significant, but not limited to the low-frequency region. The error in intensity for the custom probe, which has a reasonably flat phase mismatch of 0.05 radians (2.86°), agrees with the general trend seen in figure 4-11 and figure 4-12.

Finally, another error in measurement can be attributed to the calibration process of the two probes. The GRAS 50AI probe is calibrated using a pistonphone that outputs 250 Hz wave at 124 dB, while the custom probe microphones are calibrated using CAL200 that outputs a 1000 Hz wave at 94 dB. Calibrating at separate frequencies can pose a problem when comparing the two as the performance of each microphone at the other's calibration frequency may be unknown and consequently, outputs from the two sets of microphones for the same input may be dissimilar.

The array microphones used in the custom probe can exhibit a ± 0.5 dB error in the bandwidth used for measurement here – 562 Hz to 3548 Hz. The GRAS probe may also have a similar frequency dependent sensitivity error. Both of these may also have contributed to the difference in intensity values seen in figure 4-7 and figure 4-10.

5 Conclusion

Sound intensity measurement techniques were evaluated and a need for less expensive intensity probe was identified. The use of in-house phase correction between channels helped optimize the intensity measurements while saving on costs. While commercial probes depend on sophisticated hardware for their precision, low-cost hardware and data acquisition systems were used in conjunction with a dedicated LabVIEW code and phase calibrator to save on costs and compensate for the precision. Rapid prototyping further helped in bringing down the cost. While a commercial sound intensity probe may cost the user upwards of \$10,000, the custom probe was built for about \$1700. Additionally, the comparison between the test results from the two probes showed good agreement (± 1 dB in octave-bands).

The entire setup of the custom intensity probe used to make measurements cost approximately \$1700 using parts in our laboratory. However, this cost could be reduced further (to \sim \$100) by using a computer sound card for the data acquisition system and using low-cost MEMS microphones instead of the $\frac{1}{4}$ " ICP sensors used here. And since the accuracy of the setup depends more on the software (LabVIEW code) than the sophistication of the hardware, reasonable precision can still be expected using commercial-off-the-shelf (COTS) audio hardware.

6 Reference List

- [1] F. Jacobsen, V. Cutanda, and P. M. Juhl, "A numerical and experimental investigation of the performance of sound intensity probes at high frequencies," *The Journal of Acoustical Society of America*, vol. 103, no. 2, pp. 953-961, 1998.
- [2] P. S. Watkinson and F. J. Fahy, "Characteristics of microphone arrangements for sound intensity measurement," *Journal of Sound and Vibration*, vol. 94, no. 2, pp. 299-306, 1984.
- [3] F. Jacobsen and H.-E. d. Bree, "A comparison of two different sound intensity measurement principles," *The Journal of Acoustical Society of America*, vol. 118, no. 3, pp. 1510-1517, 2005.
- [4] M. P. Waser and M. J. Crocker, "Introduction to the Two-Microphone Cross-Spectral Method of Determining Sound Intensity," *Noise Control Engineering Journal*, vol. 22, no. 3, pp. 76-85, // 1984.
- [5] J. Y. Chung, "Cross-spectral method of measuring acoustic intensity without error caused by instrument phase mismatch," *The Journal of Acoustical Society of America*, vol. 64, no. 6, pp. 1613-1616, 1978.
- [6] F. J. Fahy, "Measurement of acoustic intensity using the cross-spectral density of two microphone signals," *The Journal of Acoustical Society of America*, vol. 62, no. 4, pp. 1057-1059, 1977.
- [7] G. P. Mathur, "A general theoretical formulation for acoustic intensity method using two microphones," *INTER-NOISE and NOISE-CON Congress and Conference Proceedings*, vol. 1983, no. 1, pp. 349-354, 1983.
- [8] G. Rasmussen, "Measuring Sound Intensity," presented at the West Coast International Meeting, San Francisco, California, 1982. Available: <https://doi.org/10.4271/820962>
- [9] F. Jacobsen and E. S. Olsen, "The influence of microphone vents on the performance of sound intensity probes," *Applied Acoustics*, vol. 41, no. 1, pp. 25-45, 1994.
- [10] A. C. Balant, J. G. C. Maling, and D. M. Yeager, "Measurement of Blower and Fan Noise Using Sound Intensity Techniques," *Noise Control Engineering Journal*, vol. 33, no. 2, pp. 77-88, // 1989.

- [11] G. Krishnappa, "Cross-spectral method of measuring acoustic intensity by correcting phase and gain mismatch errors by microphone calibration," *The Journal of Acoustical Society of America*, vol. 69, no. 1, pp. 307-310, 1981.
- [12] F. Jacobsen, "A simple and effective correction for phase mis-match in intensity probes," *Applied Acoustics*, vol. 33, no. 3, pp. 165-180, 1991.
- [13] E. Frederiksen and O. Schultz, *Pressure Microphones for Intensity Measurements with Significantly Improved Phase Properties* (Brüel & Kjær Technical Review). 1986, pp. 11-23.